Peptide-based probes for protein N-Methyltransferases

Zhang, Y.

Chapter 2

Transition state analogues as inhibitors of PRMTs

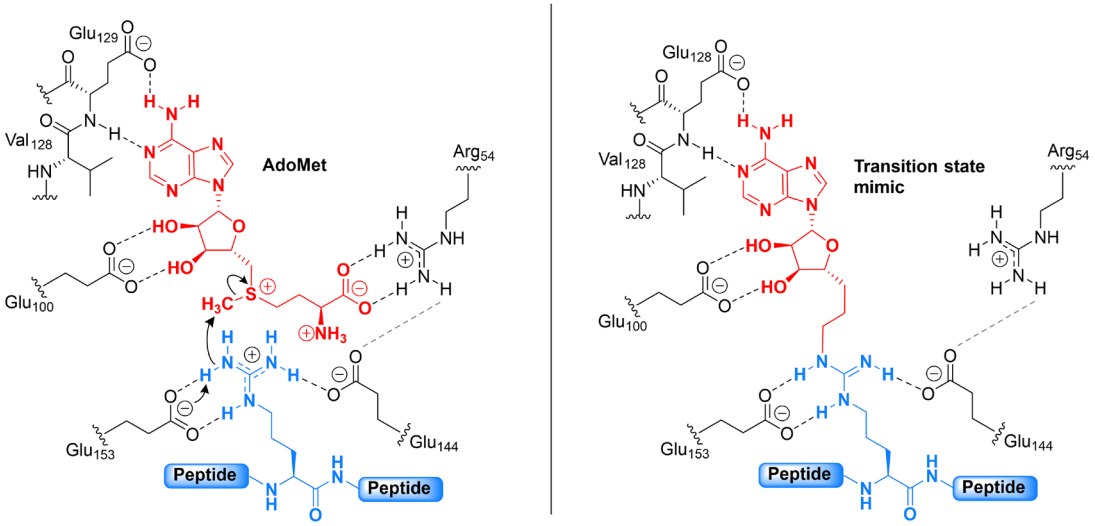

Published in

Methods **(2020)**

DOI: 10.1016/j.ymeth.2019.08.003

Abstract

Protein arginine N-methyltransferases (PRMTs) methylate arginine residues in target proteins using the ubiquitous methyl donor S-adenosyl-L-methionine (AdoMet) as a cofactor. PRMTs play important roles in both healthy and disease states and as such inhibition of PRMTs has gained increasing interest. A primary challenge in the development of PRMT inhibitors is achieving specificity for the PRMT of interest as the active sites are highly conserved for all nine members of the PRMT family. Notably, PRMTs show very little redundancy in vivo due to their specific sets of protein substrates. However, relatively little is known about the interactions of PRMTs with their protein substrates that drive this substrate specificity. We here describe the extended application of a methodology recently developed in our group for the production of peptide-based transition state mimicking PRMT inhibitors. Using this approach, an adenosine moiety, mimicking that of the AdoMet cofactor, is covalently linked to the guanidine side chain of a target arginine residue contained in a peptidic fragment derived from a PRMT substrate protein. Using this approach, histone H4 tail peptide-based transition state mimics were synthesized wherein the adenosine group was linked to the Arg3 residue. H4R3 is a substrate for multiple PRMTs, including PRMT1 and PRMT6. The inhibition results obtained with these new H4-based transition state mimics show low micromolar IC_{50} values against PRMT1 and PRMT6, indicating that the methodology is applicable to the broader family of PRMTs.

Introduction

The methylation of arginines in proteins is performed by the family of protein arginine N-methyltransferases (PRMTs). The family consists of nine members which are classified into three categories; type I PRMTs, which form asymmetrically dimethylated arginine (aDMA), type II PRMTs, which form symmetrically dimethylated arginine (sDMA) and the much less common type III PRMTs which only form monomethylated arginine (MMA). Within these categories the members are differentiated by their protein substrate specificity and cellular localizations.[1,2] In common with the majority of small molecule and peptide methyltransferase the PRMTs employ the ubiquitous methyl donor S-adenosyl-L-methionine (AdoMet) as a cofactor. In all PRMTs the methylation of the target arginine residue is facilitated by the presence of two conserved glutamate residues that serve to lock the guanidine moiety in close proximity to the AdoMet cofactor's methyl group.[3] These features in PRMT enzymes result in a highly conserved active site configuration (Figure. 1A).

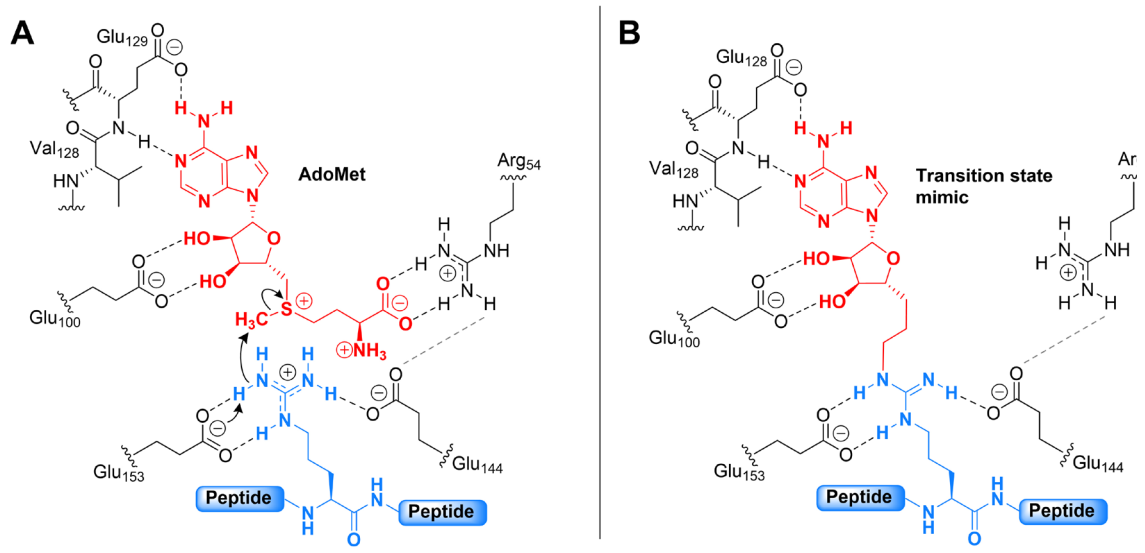

Figure. 1. A) Schematic representation of the conserved residues in the PRMT active site interacting with the AdoMet cofactor (in red) and the guanidine of the target arginine residue (in blue) (PRMT1 numbering). B) The design of the transition state mimics is based on the covalent linkage of the adenosine group (as shown in red) to the arginine sidechain in a peptide (as shown in blue). This approach leads to binding interactions with the conserved active site residues of both the AdoMet cofactor and peptide substrate binding pockets.

PRMTs are involved in a variety of cellular functions in both healthy and disease states. Cellular functions include the regulation of gene transcription, nuclear transport, DNA repair, protein-protein interactions and RNA processing.[4,5] Upon methylation of histone tails, gene transcription can be activated or repressed, depending on the arginine residue and the type of methylation (aDMA or sDMA).[6]

Notably, most PRMTs are implicated in one or more types of cancer and inhibition of PRMTs has been shown to inhibit cancer cell growth.[7] In addition, several studies have indicated the involvement of PRMTs in cardiovascular disease,[8,9] pulmonary disease [10,11] and viral infection.[12,13] Therefore, the development of inhibitors against PRMTs has gained interest over the past decade as also evidenced by recently initiated clinical trials initiated with inhibitors against PRMT5 for the treatment of solid tumours and non-Hodgkin's lymphoma.[14]

A major challenge in the development of PRMT inhibitors is how to achieve specificity for a given PRMT considering the highly conserved active site architecture shared among all members of this methyltransferase family. To this end, technologies that can provide new insights into PRMT-substrate interactions can be of great value. We here describe such an approach wherein known PRMT substrate peptides are converted into PRMT specific inhibitors. In an attempt to obtain general PRMT inhibitors, we previously synthesized a series of small molecule bisubstrate compounds with a guanidine group attached to the adenosine unit with different linker lengths.[15] For these compounds, we observed surprising selectivity among the PRMTs tested. Building on those results, we hypothesized that enhanced specificity could be achieved by linking the adenosine unit to the target arginine residue of a given PRMT substrate peptide (Figure. 1B). The adenosine-peptide conjugates mimic the transition state of the first methylation step, making the approach applicable to all three types of PRMTs. In addition, by binding in the protein substrate binding pocket, more information could be gathered about the binding interactions of the PRMTs with their (specific) protein substrates.

This approach was initially validated on coactivator-associated arginine methyltransferase 1 (CARM1 also known as PRMT4).[16] Transition state analogues were prepared based on a peptide sequence of its known substrate PABP1. Biochemical evaluation showed nanomolar inhibition against CARM1 with up to 300-fold selectivity over PRMT1. Subsequent co-crystallization experiments quickly led to high resolution crystal structures of CARM1 bound to the transition state analogue revealing the interactions in both the cofactor's and peptide binding sites. The fact that the crystals of the complex were readily obtained was attributed to the stabilizing effect the transition state mimics have on the enzyme by binding in the different substrate binding pockets simultaneously.

Following up on our promising initial results with transition state analogues designed for CARM1, we here describe the application of a similar approach for generating transition state mimics as inhibitors of PRMT1. PRMT1 is the most abundant PRMT and it is estimated that 85% of all methylated arginine residues in the proteome are methylated by PRMT1.[4,17] PRMT1 preferentially methylates the

RGG motif in target proteins and is found primarily in the cytoplasm. Alternative splicing variants show different activities, substrate specificity and cellular localizations.[18] PRMT1 substrates are diverse and include histones (H2AR3 and H4R3), splicing factors, DNA damage proteins, RNA-binding proteins, transcription factors, viral proteins and signaling proteins.[2,7] As a player in human disease, PRMT1 is overexpressed in different types of cancer[19] and is further involved in pulmonary disease[20] and cardiovascular disease.[21,22] A well-known substrate of PRMT1 is Arg^3 on the histone H4 tail (H4R3), which is often used as a marker in studies concerning the role of PRMT1.[7,23] The design of the compounds here described focuses on H4R3. As this residue is also a substrate of several other PRMTs (at least in vitro) we additionally included PRMT6 in the biochemical evaluation of the new H4R3 based transition state analogues. In contrast with PRMT1, PRMT6 is exclusively found in the nucleus.[1]

Similar to PRMT1, it preferentially methylates the RGG motif and known substrates include histone tails (H2AR3, H2AR29, H3R2, H3R8, H3R42 and H4R3), chromatin proteins, DNA-binding proteins and viral proteins.[2,24] PRMT6 is overexpressed in bladder, lung and prostate cancer and associated with pulmonary disorders.[7,11,25] Interestingly, PRMT6 is reportedly downregulated in melanoma and reduces HIV-1 production and viral replication.[26-28]

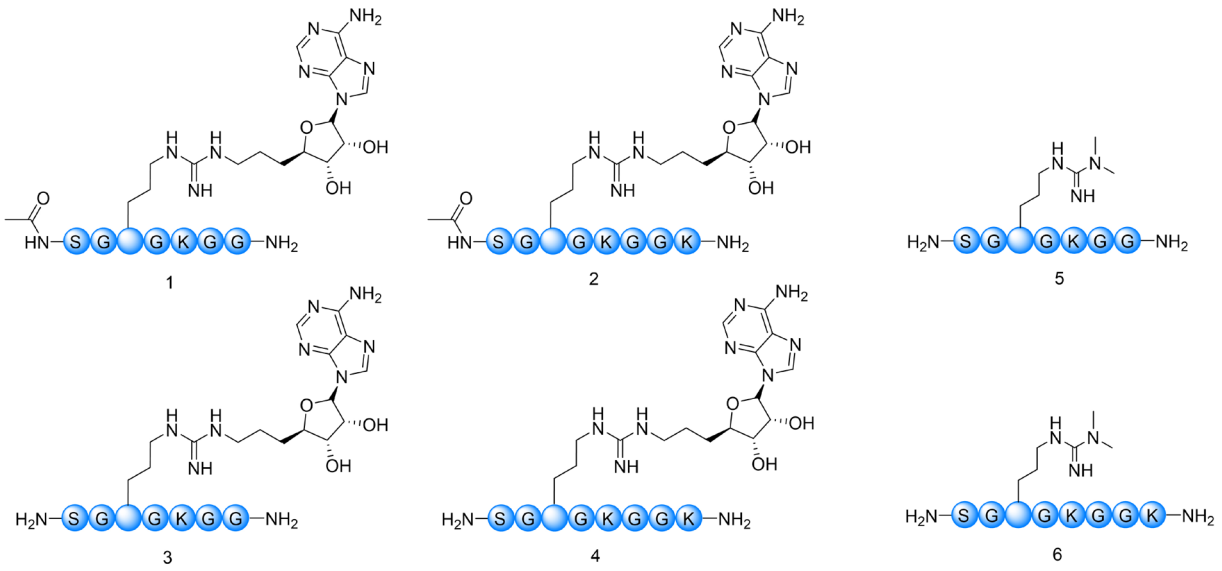

Figure. 2. Schematic representations of the structures of compounds 1–6. Compounds 1, 2 and 5 are based on residues 1–7 of the histone H4 tail and compounds 3, 4 and 6 are based on residues 1–8 of the histone H4 tail.

Above all, for installation of the adenosine unit a fully saturated three-carbon spacer was used to link to the arginine side-chain. This linker was found to be most effective among the small molecule bisubstrate inhibitors tested against PRMT1

and PRMT6 in previous work.[15] As a control we also prepared the corresponding asymmetrically dimethylated arginine containing peptides of sequences $H4^{1–7}$ (5) and $H4^{1–8}$ (6). The structures of peptides 1–6 are presented in Figure. 2.

Results and discussion

We here describe methodology for the synthesis of PRMT1 inhibiting transition state mimics through the covalent linkage of the adenosine moiety to PRMT1 target peptides. Using chemistry developed in our group,[29] the adenosine moiety can be conveniently linked to the arginine side chain of any target peptide, making the methodology widely applicable to the entire family of PRMTs.

The design of the H4R3-based transition state analogues here described is based on the N-terminal 7 or 8 amino acids of the H4 tail peptide. Because the target arginine is close to the N-terminus, the N-terminal serine residue was evaluated as both the free amine as well as in its acetylated form to investigate the effect of the N-terminus on the inhibitory activity of the modified peptides. The sequences designed around H4R3 were selected on the basis of the kinetic data on methylation of the histone H4 tail by PRMT1 as reported by Thompson and coworkers.[30] The results of their study revealed that the best catalytic efficiency was achieved with a sequence of histone 4 covering the first 21 residues ($H4^{1–21}$). A slight reduction in turnover was found for two mid-sequence truncations of $H4^{1–21}$ where either residues 11–13 or 9–15 were eliminated. Conversely, sequences $H4^{1–13}$ and $H4^{1–15}$ showed a greatly reduced methylation rate. These findings suggest that binding of the H4 tail is driven by two contributing parts: one part that interacts at the methylation site (residues 1–8) and one part that binds at a more distal binding pocket containing several negatively charged residues. Without the positive residues ($H4^{16–21}$) to bind in this negatively charged region of the enzyme, 'linker residues' 9–15 seem to hinder more than attribute to the methylation process. Therefore, sequences $H4^{1–7}$ and $H4^{1–8}$ were selected with a C-terminal amide and both a free or acetylated N-terminus. The rationale for examining the $H4^{1–7}$ peptide in addition to the $H4^{1–8}$ peptide was to elucidate the contribution of the Lys^8 residue in binding.

The methodology here described provides a flexible and generally applicable approach for the preparation of transition state analogues of PRMTs based on peptidic fragments of their respective protein substrates. By using an orthogonally protected ornithine residue at the position of the target arginine, the peptides can be synthesized by SPPS and modified on the resin. Conveniently, given that the intermediate peptides are manipulated on resin, no intermediate purification steps are necessary and all reagents can simply be washed away. Also of note is the possibility of using this approach to specifically modify a single arginine reside

when synthesizing peptides containing multiple arginines.

Key to this methodology is thiourea building block 13 that can be prepared in six steps with good to excellent yields, the details of which are presented in the supplementary information. For groups interested in applying this methodology the building block is also available on request. Also of note, if desired, variants of the thiourea building block can also be prepared with either a two-carbon spacer or an unsaturated three-carbon spacer, as we have previously described.[16]

Table 1. Inhibitory activity of compounds 1–6 against PRMT1 and PRMT6.

Compound	Sequence	IC_{50} values (μM)[a]	
		PRMT 1	PRMT 6
1	H_2N-SGR*GKGG-$CONH_2$	2.51 ± 0.24	4.82 ± 0.96
2	AcNH-SGR*GKGG-$CONH_2$	5.36 ± 0.52	10.98 ± 2.25
3	H_2N-SGR*GKGGK-$CONH_2$	4.66 ± 0.65	2.26 ± 0.72
4	AcNH-SGR*GKGGK-$CONH_2$	1.33 ± 0.25	1.22 ± 0.34
5[b]	H_2N-SGR(aDMA)GKGG-$CONH_2$	> 50	> 50
6[b]	H_2N-SGR(aDMA)GKGGK-$CONH_2$	> 50	> 50

[a] IC_{50} values from duplicate data obtained from seven concentrations ± standard deviations. The R* indicates the position where the adenosine group is incorporated. [b] In compounds 5 and 6, the central arginine residue is present in asymmetrically dimethylated form. The full IC_{50} curves were shown in the Appendix I

As reported in Table 1, compounds 1–4 display low micromolar inhibition against both PRMT1 and PRMT6. $H4^{1-7}$ analogues 1 and 2 show a 2-fold higher potency against PRMT1 over PRMT6. In addition, the free N-terminus in 1 results in slightly higher inhibition than the acetylated N-terminus in 2. For $H4^{1-8}$ analogues 3 and 4 the findings are the opposite of those found for compounds 1 and 2. Compound 3 is slightly more active against PRMT6 over PRMT1, but no significant difference is observed for compound 4 between PRMT1 and 6. Against both enzymes, the acetylated peptide 4 is more active than peptide 3 with a free N-terminus. Notably, no significant inhibition was observed for the asymmetrically dimethylated control peptides 5 and 6 when tested at 50 μM, indicating that the inhibitory activity observed for 1–4 is driven by the incorporation of the adenosine moiety. To gain additional insight into the binding of these transition state analogues to both PRMT1 and PRMT6, structural studies are now underway the results of which will be presented in due course.

As previously reported,[16] a key advantage of the methodology here presented

is that the transition state analogues can be used to facilitate co-crystallization of PRMTs with mimics of their protein substrates without the need for a cofactor analogue. Obtaining crystal structures of PRMTs bound to their peptidic substrate can give valuable insight into the interactions in the binding site of the peptide substrate, providing information that is crucial for the development of selective small molecule inhibitors. It is known that the co-crystallization of PRMTs with their substrates is often very challenging due to the necessity of including an analogue of the AdoMet cofactor. AdoMet itself cannot be used as this would result in the formation of the (di-)methylated product. Often AdoMet analogues S-adenosyl-L-homocysteine (AdoHcy), the product of the methylation reaction, or sinefungin are used to obtain structures of the ternary complex of enzyme, cofactor and substrate. However, the use of AdoHcy in co-crystallization studies of PRMTs is limited for obtaining mechanistical insight as it would only stabilize the PRMT in the conformation it adopts after the methyltransfer takes place. In addition, other AdoMet analogues introduce unnatural interactions into the active site, the effects of which can be difficult to interpret. Furthermore, the crystallization of a ternary complex is often more challenging than for a binary complex of substrate and enzyme. This is evidenced by the limited number of structures of PRMTs bound to their protein substrate. In fact, for only CARM1 and PRMT5 have high resolution crystal structures been reported that show the peptide substrate bound to the enzyme.[16,31,32] In the only structure published to date for PRMT1 bound to a substrate peptide only the target arginine residue was resolved in the active site while in similar studies with PRMT7 only the target arginine glycine segment of a larger substrate peptide was visible.[33,34]

In conclusion, the results of compounds 1–6 show that our peptide transition state analogue methodology is generally applicable throughout the family of PRMTs. Where previous studies focused on PRMT4, we here demonstrate the applicability of the methodology in generating peptide based bisubstrate inhibitors for PRMT1 and PRMT6 as well. Future efforts will be directed to examining the applicability of peptides 1–4 in co-crystallization studies with PRMT1 and 6 as well as further application of the methodology towards other PRMTs.

Experimental Procedures

Materials and methods

All reagents employed were of American Chemical Society (ACS) grade or finer and were used without further purification unless otherwise stated. The Pbf-thiourea building block and its precursors 8-13 were synthesized according to previously described procedures.[15,16] All known compounds prepared had NMR spectra and HRMS data consistent with the assigned structures. All reactions and fractions

from column chromatography were monitored by thin layer chromatography (TLC) using plates with a UV fluorescent indicator (normal SiO_2, Merck 60 F 254). One or more of the following methods were used for visualization: UV absorption by fluorescence quenching; phosphomolybdic acid: ceric sulfate: sulfuric acid: H_2O (10 g:1.25 g: 12 mL:238 mL) staining; $KMnO_4$ staining; PPh_3 staining; ninhydrin staining. Flash chromatography was performed using Merck type 60, 230–400 mesh silica gel.

The final compounds 1-6 were purified by preparative HPLC performed on a BESTATechnik system with a Dr. Maisch Reprosil Gold 120 C18 column (25 × 250 mm, 10 µm) and equipped with a ECOM Flash UV detector monitoring at 214 nm. Compounds were eluted with a water–methanol gradient moving from 0% to 100% methanol (0.1% TFA) over 60 minutes at a flow-rate of 12.0 mL·min^{-1} with UV detection at 214 nm. Purity of compounds 1-4 was confirmed to be ≥95% by HPLC. HPLC analyses were performed on a Shimadzu Prominence-i LC-2030 system with a Dr. Maisch ReproSil Gold 120 C18 column (4.6 × 250 mm, 5 or 10 µm) at 30°C and equipped with a UV detector monitoring at 214 and 254 nm. Compounds were eluted with a water– methanol gradient moving from 0% to 100% methanol (0.1% TFA) over 50 minutes at a flow rate of 1.0 mL·min^{-1} with UV detection (214 nm and 254 nm). Compounds 5 and 6 were analyzed on a Shimadzu LC-20AD system with a Shimadzu Shim-Pack GIST-AQ C18 column (3.0 x 150 mm, 3 µm) at 30°C and equipped with a UV detector monitoring at 214 and 254 nm. This system was connected to a Shimadzu 8040 triple quadrupole mass spectrometer (ESI ionization). Compounds were eluted with a water–methanol gradient moving from 0% to 100% methanol (0.1% FA) over 15 minutes at a flow rate of 0.5 mL·min^{-1} with UV detection (214 nm and 254 nm) and MS detection.

HRMS analyses were performed on a Thermo Scientific Dionex UltiMate 3000 HPLC system with a Phenomenex Kinetex C18 column (2.1 x 150 mm, 2.6 µm) at 35 °C and equipped with a diode array detector. The following solvent system, at a flow rate of 0.3 mL min^{-1}, was used: solvent A, 0.1 % formic acid in water; solvent B, 0.1% formic acid in acetonitrile. Gradient elution was as follows: 95:5 (A/B) for 1 min, 95:5 to 5:95 (A/B) over 9 min, 5:95 to 2:98 (A/B) over 1 min, 2:98 (A/B) for 1 min, then reversion back to 95:5 (A/B) over 2 min, 95:5 (A/B) for 1 min. This system was connected to a Bruker micrOTOF-Q II mass spectrometer (ESI ionisation) calibrated internally with sodium formate.

Synthesis of the building block. Installation of the adenosine moiety at the target arginine residue in the peptides prepared required access to a specific thiourea building block (Compound 13, Scheme 1), The preparation of this thiourea begins from commercially available 2,3-O-isopropylidine adenosine alcohol 7 as we previously reported.[16] Briefly, 7 is first transformed into unsaturated ethyl ester 8 in

a one-pot oxidation and Wittig reaction. Subsequently, the ester is reduced to alcohol 9 using diisobutylaluminium hydride (DiBAL-H). The alcohol is converted to phthalimide-protected amine 11 via a Mitsunobu reaction with phthalimide and subsequent deprotection using methylamine resulting in amine 12. The amine is then reacted with 2,2,4,6,7-pentamethyldihydrobenzofuran-5-sulfonyl isothiocyanate (Pbf-NCS) [29] to form the Pbf-protected thiourea building block 13.

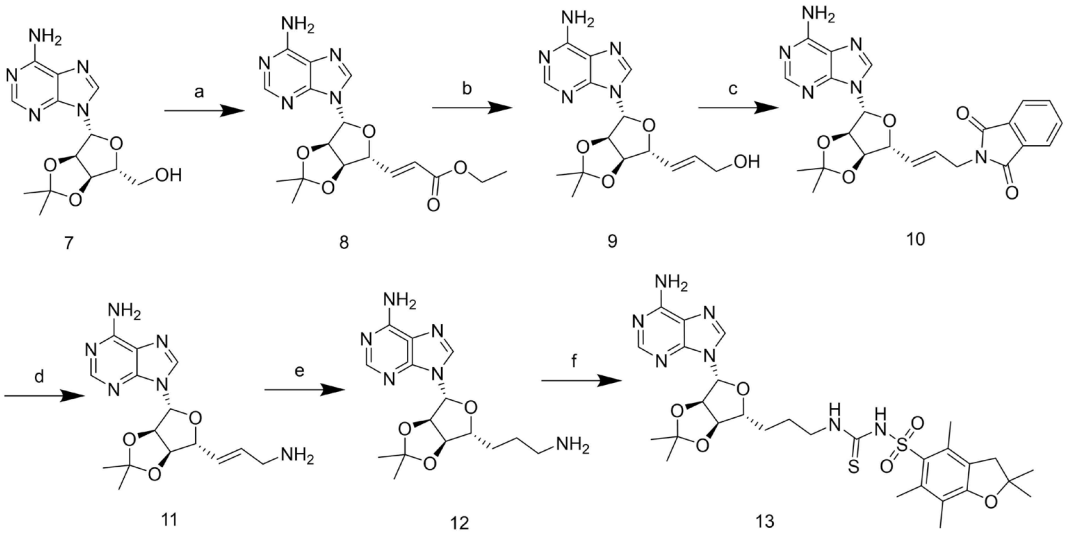

Scheme 1. Synthesis of Pbf-protected thiourea building block 13. Reagents and conditions: (a) IBX, $Ph_3P{=}CHCO_2Et$, DMSO, 79%; (b) DIBAL-H, hexane, DCM, 78%; (c) phthalimide, PPh_3, diethyldiazocarboxylate, THF, 94%; (d) $MeNH_2$, EtOH, 94%; (e) 10% Pd/C, H_2 (g), EtOH, 98%; (f) Pbf-NCS, Et_3N, DCM, 83%.

Ethyl-(E)-3-((3aR,6R,6aR)-6-(6-amino-9H-purin-9-yl)-2,2-dimethyltetrahydrofuro[3,4-d][1,3]dio xol -4-yl)acrylate (8)

2′,3′-O-isopropylideneadenosine 7 (12.3 g, 40 mmol) was dissolved in DMSO (100 mL) and 2-iodoxybenzoic acid (IBX) (27.8 g, 100 mmol) and $Ph_3P{=}CHCOOC_2H_5$ (42.8 g, 100 mmol) were added. The mixture was stirred at room temperature for 72 h. Water (500 mL) was added and the mixture was extracted with EtOAc (2 × 500 mL). The combined organic layers were dried with Na_2SO_4, the mixture was concentrated and purified by column chromatograph (4% MeOH in EtOAc) to give compound 8 (11.9 g, 79%) as a white powder.

(E)-3-((3aR,6R,6aR)-6-(6-amino-9H-purin-9-yl)-2,2-dimethyltetrahydrofuro[3,4-d][1,3]dioxol-4-yl)prop-2-en-1-ol (9)

Compound 8 (4.5 g, 12 mmol) was dissolved in DCM (30 mL), then cooled down to -78°C and a 1 M solution of DIBAL-H in hexane (100 mL) was added dropwise. The mixture was stirred at -78°C for 2 h and then quenched with MeOH (65 mL). A saturated aqueous solution of potassium sodium tartrate monohydrate (Rochelle

salt, 550 mL) was added and the resulting suspension was stirred vigorously at room temperature overnight, then extracted with EtOAc (2 × 500 mL). The combined organic phases were dried (Na_2SO_4) and concentrated. The crude was purified by column chromatograph (4-6% MeOH gradient in EtOAc) to give compound 9 (3.1 g, 78%) as a white powder.

2-((E)-3-((3aR,6R,6aR)-6-(6-amino-9H-purin-9-yl)-2,2-dimethyltetrahydrofuro[3,4-d][1,3]dioxol -4-yl)allyl)isoindoline-1,3-dione (10)

To a solution of compound 9 (2.4 g, 7 mmol) in THF (60 ml), phthalimide (1.0 g, 7 mmol) and Ph_3P (1.8 g, 7 mmol) were added. DEAD (1.3 ml, 7 mmol) was added dropwise to a stirred suspension of mixture. After stirring for 2 h at room temperature during which a colorless solid started to precipitate. Stirring was continued for 1 h, after which the mixture was cooled to 0°C for 30 minutes and the product was filtered off. The residue was washed with Et_2O (3 × 50 mL) and dried in vacuum to give 10 (3.1 g, 94%) as white powder.

9-((3aR,4R,6aR)-6-((E)-3-aminoprop-1-en-1-yl)-2,2-dimethyltetrahydrofuro[3,4-d][1,3]d ioxol -4-yl)-9H-purin-6-amine (11)

To compound 10 (1.5 g, 3.2 mmol) was dissolved in a solution of 33% CH_3NH_2 in ethanol and the mixture was stirred at room temperature overnight. The mixture was concentrated, and redissolved in chloroform (40 mL) and extracted with 10% acetic acid (50 mL). The aqueous phase was washed with chloroform (3 × 40 mL), then adjusted adjusted with 2N NaOH to pH >12 and extracted with chloroform (4 × 40 mL). The combined organic phases were dried (Na_2SO_4) and concentrated to give 11 (990 mg, 94%) as white powder.

9-((3aR,4R,6aR)-6-(3-aminopropyl)-2,2-dimethyltetrahydrofuro[3,4-d][1,3]dioxol-4-yl)-9H-purin-6-amine (12)

To a solution of compound 11 (880 mg, 2.6 mmol) in methanol (20 mL), water (5 mL) and acetic acid (5 drops), Pd-C (20 wt%, 90 mg) was added and the mixture was stirred overnight under a hydrogen atmosphere until MS showed complete conversion. The mixture was filtered through celite, washed with methanol, and concentrated to give 12 (870 mg, 98%) a yellow solid.

N-((3-((3aR,6R,6aR)-6-(6-amino-9H-purin-9-yl)-2,2-dimethyltetrahydrofuro[3,4-d][1,3]dioxol-4-yl)propyl)carbamothioyl)-2,2,4,6,7-pentamethyl-2,3-dihydrobenzofuran-5-sulfon amide (13)

Compound 12 (670 mg, 2 mmol) was dissolved in DCM (10 mL) and cooled to 0

°C. Trimethylamine (0.56 mL, 4 mmol) was added, followed by dropwise addition of a 0.1 M solution of Pbf-NCS (24 mL, 2.4 mmol) in DCM. After 75 min, the mixture was diluted with DCM (100 mL) and washed with water (3 × 75 mL) and brine (3 × 75 mL), dried with Na_2SO_4 and concentrated. The crude was purified by column chromatograph (2-4% MeOH gradient in DCM) to give compound 13 (1.1 g, 83%) as a white powder.

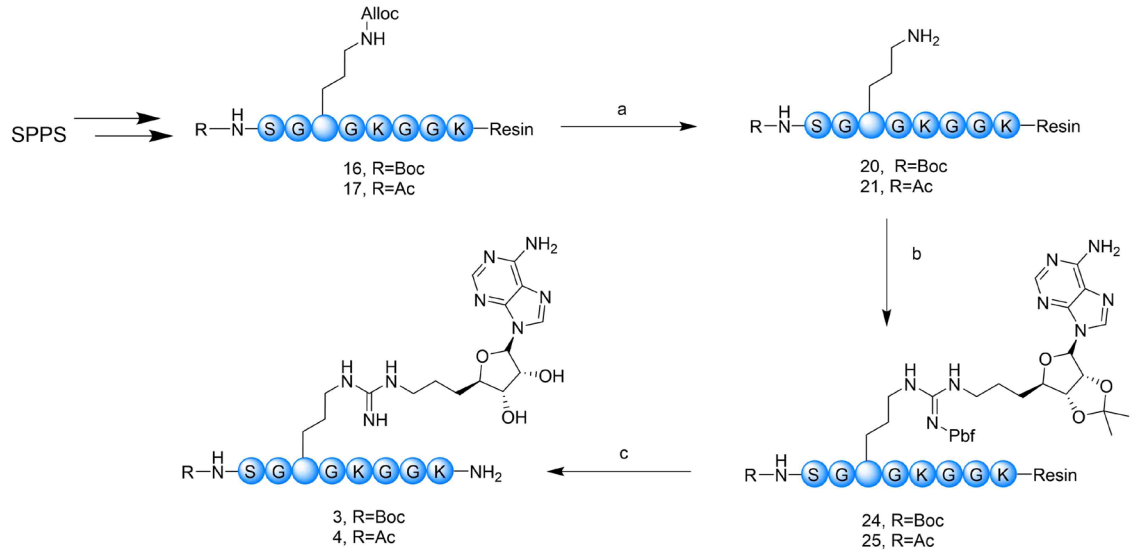

Scheme 2. On-resin modification procedure for the synthesis of transition state analogues 1–4, presented for H4[1–8] peptides 3 and 4. The H4[1–7] peptides 1 and 2 were prepared following the same route. Reagents and conditions: a) $Pd(PPh_3)_4$, phenylsilane, DCM, Ar (g), dark, rt, 1 h; b) 13, EDCI, DCM, N_2 (g), rt, 90 min; c) TFA/TIPS/H_2O (95:2.5:2.5), rt, 1 h.

Peptides Synthesis. In preparing the peptides, the target arginine in the sequence was replaced by an Alloc-protected ornithine residue, which allows for orthogonal deprotection and modification of the required residue. As a representative example Scheme 2 illustrates the synthetic route used in preparing transition state mimics 3 and 4. To begin, the Alloc-protected ornithine peptides were synthesized manually following standard Fmoc solid phase peptide synthesis (SPPS) protocols using Rink Amide tentagel resin. The peptide couplings were performed in N,N-dimethylformamide (DMF) at ambient temperature for 1 h using standard Fmoc-protected amino acids with (2-(1H-benzotriazol-1-yl)-1,1,3,3-tetramethyluronium hexafluorophosphate (HBTU) as the activator and di-isopropylethylamine (DiPEA) as base. Deprotection of the Fmoc protecting group was done with 20% piperidine in DMF. Each step was checked by means of a Kaiser test [35,36] to ensure completion of the reaction. After coupling and Fmoc deprotection of the last residue the resin was split and one half treated with di-tert-butyldicarbonate (Boc_2O) to generate resin bound intermediate 16 while the other half was acetylated with acetic anhydride to yield intermediate 17. Resin bound 16 and 17 were subsequently converted to the corresponding adenosine-linked arginine peptides

On-resin installation of the adenosine unit. The on-resin conjugation of the adenosine thiourea building block (13) to the peptides is described here for the synthesis of compounds 3 and 4. The same procedure is used to synthesize compounds 1 and 2.

Peptides were Alloc-deprotected on the resin using tetrakis(triphenylphosphine)-palladium(0) and phenylsilane in DCM. The mixture was shaken for 1 hour under argon atmosphere and protected from light. Upon completion of deprotection, the resin is drained, washed with DCM (5 × 10 mL), 0.5% diethyldithiocarbamic acid sodium salt (5 × 10 mL), DMF (5 × 10 mL) and DCM (5 × 10 mL). Subsequently, the adenosine thiourea building block 13 (105 mg, 0.13 mmol, 1.3 eq) was coupled to the free amine using 1-ethyl-3-(3-dimethylaminopropyl)- carbodiimide (EDCI) (34.5 mg, 0.15 mmol, 1.5 eq) in DMF (10 mL) for 1.5 hours at room temperature. The mixture was drained and the resin was washed with DCM (3×10 mL), DMF (3×10 mL) and DCM (2×10 mL). Finally, the peptides were deprotected and cleaved from the resin using a standard cleavage cocktail of TFA/TIPS/H_2O (95:2.5:2.5). Precipitation in MTBE/hexane (1:1) yielded the crude peptide, which was purified by preparative HPLC. The purity and identity were confirmed by analytical HPLC and High-resolution Mass Spectrometry.

Synthesis of aDMA-peptides 5 and 6. Asymmetrically dimethylated arginine (aDMA) - containing peptides 5 and 6 were synthesized on a CEM Liberty Blue™ Automated Microwave Peptide Synthesizer. Peptide couplings were performed by using Fmoc-protected amino acid (4.0 eq), Oxyma (8.0 eq) and DIC (4.0 eq) in DMF (5 mL). Each coupling took 2 minutes at 90°C, followed by Fmoc deprotection using 20% piperidine in DMF for 4 minutes at 90°C. Special building block Fmoc-Adma(Pbf)-OH was coupled at room temperature overnight using 2 equivalents of amino acid.

After completion of the peptide synthesis, the peptides were deprotected and cleaved from the resin using a standard cleavage cocktail of TFA/TIPS/H2O (95:2.5:2.5). Precipitation in MTBE/hexane (1:1) yielded the crude peptide, which was purified by preparative HPLC. The purity and identity were confirmed by analytical HPLC and High-resolution Mass Spectrometry.

Biochemical evaluation. Methyltransferase inhibition assays were performed using commercially available chemiluminescent assay kits for PRMT1 and PRMT6 (BPS Bioscience, San Diego, CA, USA). The inhibition reactions were performed in duplicate at room temperature for 1 h using 96-well plates precoated with histone $H4^{1–24}$ peptides as the substrate in a total volume of 50 µl containing proprietary assay buffer, 20 µM AdoMet, enzyme: PRMT1 (10 ng per reaction) and PRMT6 (200 ng per reaction) and inhibitors with concentration ranges of 0.0128–200 µM

in water. Positive controls were performed by addition of pure water instead of inhibitor solution. Blank and substrate controls were conducted in the absence of enzyme and AdoMet, respectively. After incubation for 1 h at room temperature, the wells were washed and blocked, primary antibody was added to each well and incubated for an additional 1 h. After washing and blocking, a secondary HRP-labelled antibody was added and incubated for another 30 min. After a final washing and blocking step, the HRP-substrate mixture was added to the wells and the luminescence was measured immediately using a Tecan spark plate reader. All the measurements were performed in duplicate and the luminescence data analysed using GraphPad Prism 7. Blank data was subtracted from the luminescence data and the results were subsequently normalized with the highest value in the concentration range defined as 100% inhibition. The percentage of inhibition activity was plotted as a function of inhibitor concentration and fit using non-linear regression analysis of the sigmoidal dose-response curve generated using the normalized data and a variable slope following equation:

$$Y = \frac{100}{(1 + 10^{((logIC50 - X) * Hillslope))})}$$

where Y=percent activity, X=the logarithmic concentration of the compound, Hillslope=slope factor or Hill coefficient. The IC_{50} value was determined by the half maximal inhibitory concentration. The standard deviations were reported using the symmetrical CI function.

References

1. M.T. Bedford, P. Pably, C. Eckerich, F.O. Fackelmayer and F. Herrmann, Human protein arginine methyltransferases in vivo – distinct properties of eight canonical members of the PRMT family, J. Cell Sci., 2009, 122, 667–677.
2. H. Wei, R. Mundade, K.C. Lange and T. Lu, Protein arginine methylation of non-histone proteins and its role in diseases, Cell Cycle, 2014, 13, 32–41.
3. H.L. Rust, C.I. Zurita-Lopez, S. Clarke and P.R. Thompson, Mechanistic studies on transcriptional coactivator protein arginine methyltransferase 1, Biochemistry, 2011, 50, 3332–3345.
4. M.T. Bedford and S.G. Clarke, Protein arginine methylation in mammals: who, what, and why, Mol. Cell, 2009, 33, 1–13.
5. Y. Morales, T. Cáceres, K. May and J.M. Hevel, Biochemistry and regulation of the protein arginine methyltransferases (PRMTs), Arch. Biochem. Biophys., 2016, 590, 138–152.
6. A.Di Lorenzo and M.T. Bedford, Histone arginine methylation, FEBS Lett., 2011, 585, 2024–2031.
7. Y. Yang and M.T. Bedford, Protein arginine methyltransferases and cancer, Nat. Rev. Cancer, 2013, 13, 37–50.
8. S. Franceschelli, A. Ferrone, M. Pesce, G. Riccioni and L. Speranza, Biological functional relevance of asymmetric dimethylarginine (ADMA) in cardiovascular disease, Int. J. Mol. Sci., 2013, 4, 24412–24421.
9. J.E. Nahon, C. Groeneveldt, J.J. Geerling, M. van Eck and M. Hoekstra, Inhibition of protein arginine methyltransferase 3 activity selectively impairs liver X receptordriven transcription of hepatic lipogenic genes in vivo, Br. J. Pharmacol., 2018, 175, 3175–3183.
10. D. Zakrzewicz and O. Eickelberg, From arginine methylation to ADMA: a novel mechanism with therapeutic potential in chronic lung diseases, BMC Pulm. Med., 2009, 9, 1–7.
11. D. Zakrzewicz, A. Zakrzewicz, K.T. Preissner, P. Markart and M. Wygrecka, Protein arginine methyltransferases (PRMTs): promising targets for the treatment of pulmonary disorders, Int. J. Mol. Sci., 2012, 13, 12383–12400.
12. B. Xie, C.F. Invernizzi, S. Richard and M.A. Wainberg, Arginine methylation of the human immunodeficiency virus type 1 tat protein by PRMT6 negatively affects tat interactions with both cyclin T1 and the tat transactivation region, J. Virol., 2007, 81, 4226–4234.
13. S. Pileri, L. Alinari, S. Roy, E.M. Smith, B. Yu, A. De Leo, J.C. Byrd, P.L. Smith, K.V. Mahasenan, J.E. Bradner, S. Sif, T. Motiwala, J.T. Patton, J.-H. Chung, L. Ayers, L. Kim, O. Elemento, C. Li, Y. Wu, S. Majumder, S. Jacob, F. Yan, V. Karkhanis, R.A. Baiocchi, S. Chen-Kiang, C. Agostinelli, R. Lapalombella and C. Quinion, Selective inhibition of protein arginine methyltransferase 5 blocks initiation and maintenance of B-cell transformation, Blood, 2015, 125, 2530–2543.

14. Wang, W. Hu and Y. Yuan, Protein arginine methyltransferase 5 (PRMT5) as an anticancer target and its inhibitor discovery, J. Med. Chem., 2018, 21, 9429–9441.
15. M. Van Haren, L.Q. Van Ufford, E.E. Moret and N.I. Martin, Synthesis and evaluation of protein arginine N-methyltransferase inhibitors designed to simultaneously occupy both substrate binding sites, Org. Biomol. Chem., 2015, 13, 549-560.
16. M.J. van Haren, N. Marechal, N. Troffer-Charlier, A. Cianciulli, G. Sbardella, J. Cavarelli and N.I. Martin, Transition state mimics are valuable mechanistic probes for structural studies with the arginine methyltransferase CARM1, Proc. Natl. Acad. Sci., 2017, 114, 3625–3630.
17. J. Tang, P.N. Kao and H.R. Herschman, Protein-arginine methyltransferase i, the predominant protein-arginine methyltransferase in cells, interacts with and is regulated by interleukin enhancer-binding factor 3, J. Biol. Chem., 2000, 275, 19866–19876.
18. R.M. Baldwin, A. Morettin, G. Paris, I. Goulet and J. Cotéˆ ., Alternatively spliced protein arginine methyltransferase 1 isoform PRMT1v2 promotes the survival and invasiveness of breast cancer cells, Cell Cycle, 2012, 11, 4597–4612.
19. C. Poulard, L. Corbo, M and Le Romancer, Protein arginine methylation/demethylation and cancer, Oncotarget, 2016, 7, 67532–67550.
20. L. Liu, J. Sun, C. Jiang, Q. He, X. Lan, J. Tian, S. Lu, B. Zhong, R. Bao, Q. Sun, X. Yang and M. Roth, PRMT1 upregulated by epithelial proinflammatory cytokines participates in COX2 expression in fibroblasts and chronic antigen-induced pulmonary inflammation, J. Immunol., 2015, 195, 298–306.
21. J.H. Pyun, H.J. Kim, M.H. Jeong, B.Y. Ahn, T.A. Vuong, D.I. Lee, S. Choi, S.H. Koo, H. Cho and J.S. Kang, Cardiac specific PRMT1 ablation causes heart failure through CaMKII dysregulation, Nat. Commun., 2018, 9, 5017.
22. K. Murata, W. Lu, M. Hashimoto, N. Ono, M. Muratani, K. Nishikata, J.-D. Kim, S. Ebihara, J. Ishida and A. Fukamizu, PRMT1 deficiency in mouse juvenile heart induces dilated cardiomyopathy and reveals cryptic alternative splicing products, iScience, 2018, 8, 200–213.
23. Y. Feng, J. Wang, S. Asher, L. Hoang, C. Guardiani, I. Ivanov and Y.G. Zheng, Histone H4 acetylation differentially modulates arginine methylation by an in cis mechanism, J. Biol. Chem., 2011, 286, 20323–20334.
24. A.Frankel, N. Yadav, J. Lee, T.L. Branscombe, S. Clarke, M.T. Bedford, The novel human protein arginine N-methyltransferase PRMT6 is a nuclear enzyme displaying unique substrate specificity, J. Biol. Chem., 2002, 277, 3537–3543.
25. R. Henrique, P. Costa-Pinheiro, A. Pereira, J. Ramalho-Carvalho, C. Jerónimo, J. Oliveira, L. Antunes, F.D. Menezes, I. Carneiro and F.Q. Vieira, Deregulated expression of selected histone methylases and demethylases in prostate carcinoma, Endocr. Relat. Cancer, 2013, 21, 51–61.

26. K. Limm, C. Ott, S. Wallner, D.W. Mueller, P. Oefner, C. Hellerbrand and A.K. Bosserhoff, Deregulation of protein methylation in melanoma, Eur. J. Cancer, 2013, 49, 1305–1313.
27. M.-C. Boulanger, C. Liang, R.S. Russell, R. Lin, M.T. Bedford, M.A. Wainberg and S. Richard, Methylation of tat by PRMT6 regulates human immunodeficiency virus type 1 gene expression, J. Virol., 2005, 79, 124–131.
28. D.N. Singhroy, T. Mesplède, A. Sabbah, P.K. Quashie, J.P. Falgueyret and M.A. Wainberg, Automethylation of protein arginine methyltransferase 6 (PRMT6) regulates its stability and its anti-HIV-1 activity, Retrovirology, 2013, 10, 1–10.
29. N.I. Martin and R.M.J. Liskamp, Preparation of NG-substituted L-arginine analogues suitable for solid phase peptide synthesis, J. Org. Chem., 2008, 73, 7849–7851.
30. T.C. Osborne, O. Obianyo, X. Zhang, X. Cheng and P.R. Thompson, Protein arginine methyltransferase 1: positively charged residues in substrate peptides distal to the site of methylation are important for substrate binding and catalysis, Biochemistry, 2007, 46, 13370–13381.
31. Moradei, P.A. Boriack-Sjodin, A. Drew, L. Jin, M.P. Scott, S. Ribich, M.P. Moyer, C. Sneeringer, R.A. Copeland and S.L. Jacques, Structural insights into ternary complex formation of human CARM1 with various substrates, ACS Chem. Biol., 2015, 11, 763–771.
32. K. Mavrakis, E.R. McDonald, M.R. Schlabach, E. Billy, G.R. Hoffman, A. DeWeck, D.A. Ruddy, K. Venkatesan, G. McAllister, R. DeBeaumont, S. Ho, Y. Liu, Y. Yan-Neale, G. Yang, F. Lin, H. Yin, H. Gao, D.R. Kipp, S. Zhao, J.T. McNamara, E.R. Sprague, Y.S. Cho, J. Gu, K. Crawford, V. Capka, K. Hurov, J.A. Porter, J. Tallarico, C. Mickanin, E. Lees, R. Pagliarini, N. Keen, T. Schmelzle, F. Hofmann, F. Stegmeier and W.R. Sellers, Abstract LB-017: disordered methionine metabolism in MTAP/CDKN2A-deleted cancers leads to marked dependence on PRMT5, Cancer Res, 2016, 76, LB-017-LB-017.
33. X. Zhang and X. Cheng, Structure of the predominant protein arginine methyltransferase PRMT1 and analysis of its binding to substrate peptides, Structure, 2003, 11, 509–520.
34. L. Liu, C. Wang, J. Wu, X. Chen, T.B. Caceres, M. Teng, Y. Zhu, Q. Gong, J.M. Hevel Z. Zhang, Y. Shi, J. Chen, J. Peng, J. Wang and X. Zuo, Structural determinants for the strict monomethylation activity by Trypanosoma brucei protein arginine methyltransferase 7, Structure , 2014, 22, 756–768.
35. Kaiser, R.L. Colescott, C.D. Bossinger and P.I. Cook, Color test for detection of free terminal amino groups in the solid-phase synthesis of peptides, Anal. Biochem., 1970, 34, 595–598.
36. V.K. Sarin, S.B.H. Kent, J.P. Tam and R.B. Merrifield, Quantitative monitoring of solidphase peptide synthesis by the ninhydrin reaction, Anal. Biochem., 1981, 117, 147–157.